The Formation of a 70 M⊙ Black Hole at High Metallicity

Belczynski, K.; Hirschi, R.; Kaiser, E.A.; Liu, J.; Casares, J.; Lu, Y.; O'Shaughnessy, R.; Heger, A.; Justham, S.; Soria, R.

DOI
10.3847/1538-4357/ab6d77

Publication date
2020

Document Version
Submitted manuscript

Published in
Astrophysical Journal

Draft version January 14, 2020
Preprint typeset using LaTeX style emulateapj v. 12/16/11

THE FORMATION OF A 70 $M_\odot$ BLACK HOLE AT HIGH METALLICITY

K.Belczynski[1], R.Hirschi[2,3], E.A.Kaiser[3], Jifeng Liu[4,11], J.Casares[5,6], Youjun Lu[4,11], R. O'Shaughnessy[7], A.Heger[8,9], S.Justham[10,11], R.Soria[4,11]
[1] Nicolaus Copernicus Astronomical Center, Polish Academy of Sciences, ul. Bartycka 18, 00-716 Warsaw, Poland (chrisbelczynski@gmail.com)
[2] Kavli IPMU (WPI), The University of Tokyo, Kashiwa, Chiba 277-8583, Japan
[3] Astrophysics group, Keele University, Keele ST5 5BG, United Kingdom
[4] Key Laboratory of Optical Astronomy, National Astronomical Observatories, Chinese Academy of Sciences, Beijing 100101, China
[5] Instituto de Astrofísica de Canarias, c/Via Laceta s/n, E-38205 La Laguna, Tenerife, Spain
[6] Departamento de Astrofísica, Universidad de La Laguna, E-38206 La Laguna, Tenerife, Spain
[7] Rochester Institute of Technology, Rochester, New York 14623, USA
[8] School of Physics and Astronomy, Monash University, Victoria 3800, Australia
[9] OzGrav: Australian Research Council Centre of Excellence for Gravitational Wave Discovery, Clayton, VIC 3800, Australia
[10] Anton Pannekoek Institute of Astronomy and GRAPPA, University of Amsterdam, 1090 GE Amsterdam, the Netherlands
[11] School of Astronomy and Space Science, University of the Chinese Academy of Sciences, Beijing 100012, China
Draft version January 14, 2020

ABSTRACT

A 70 $M_\odot$ black hole was discovered in Milky Way disk in a long period ($P = 78.9$ days) and almost circular ($e = 0.03$) detached binary system (LB-1) with a high ($Z \sim 0.02$) metallicity 8 $M_\odot$ B star companion. Current consensus on the formation of black holes from high metallicity stars limits the black hole mass to be below 20 $M_\odot$ due to strong mass loss in stellar winds. So far this was supported by the population of Galactic black hole X-ray binaries with Cyg X-1 hosting the most massive ~ 15 $M_\odot$ black hole. Using the Hurley et al. 2000 analytic evolutionary formulae, we show that the formation of a 70 $M_\odot$ black hole in high metallicity environment is possible if stellar wind mass loss rates, that are typically adopted in evolutionary calculations, are reduced by factor of 5. As observations indicate, a fraction of massive stars ($\sim 7\%$) have surface magnetic fields which, as suggested by Owocki et al. 2016, may quench the wind mass-loss, independently of stellar mass and metallicity. We also computed detailed stellar evolution models and we confirm such a scenario. A non-rotating 85 $M_\odot$ star model at $Z = 0.014$ with decreased winds ends up as a 71 $M_\odot$ star prior core-collapse with a 32 $M_\odot$ helium core and a 28 $M_\odot$ CO core. Such star avoids pair-instability pulsation supernova mass loss that severely limits black hole mass and may form a ~ 70 $M_\odot$ black hole in the direct collapse. Stars that can form 70 $M_\odot$ black holes at high Z expand to significant size with radius of $R \gtrsim 600$ $R_\odot$ (thanks to large H-rich envelope), however, exceeding the size of LB-1 orbit (semi-major axis $a \lesssim 350$ $R_\odot$). Therefore, we can explain the formation of black holes upto 70 $M_\odot$ at high metallicity and this result is independent from LB-1; whether it hosts or does not host a massive black hole. However, if LB-1 hosts a massive black hole we are unable to explain how such a binary star system could have formed without invoking some exotic scenarios.

Subject headings: stars: black holes, neutron stars, x-ray binaries

1. INTRODUCTION

LB-1 is reported as a detached binary system containing B star with a mass of 8 $M_\odot$ ($-1.2/+0.9$ $M_\odot$) and a black hole (BH) with a mass of 68 $M_\odot$ ($-13/+11$ $M_\odot$). The binary system orbit is almost circular with $e = 0.03$ ($-0.01/+0.01$ $M_\odot$) and has an orbital period of $P_{\rm orb} = 78.9$ days ($-0.3/+0.3$ days). This corresponds to a physical semi-major axis of $a = 300 - 350$ $R_\odot$ and a Roche lobe radius of the BH $R_{\rm BH,lobe} \lesssim 200$ $R_\odot$. This system is one of the widest known binary system hosting a stellar-origin BH, see `https://stellarcollapse.org`. Two other binaries, proposed to host BH candidates, were also discovered by the radial velocity method by Thompson et al. (2019) and Giesers et al. (2018, although this is in a globular cluster and has a very large period, $P = 167$ d, and eccentric orbit with $e = 0.6$ and it must have formed by capture).

The LB-1 was discovered by the 4-meter class telescope LAMOST and the spectroscopic orbit was confirmed by the 10-meter class Gran Telescopio Canarias and Keck telescopes. Chandra non-detection places X-ray emission at the very low level $< 2 \times 10^{31}$ erg/s. An H_α emission line was observed, however, and since it follows a BH (small accretion disk around the BH from the B star wind) the double spectroscopic orbital solution was obtained. The system is on the outskirts of the Galactic disk, in the anti-Galactic center direction, about 4 kpc away from Sun. There is no globular cluster nearby (< 4kpc). The chemical composition of B star indicates a slightly over-Solar metal abundance $Z = 0.02$ assuming $Z_\odot = 0.017$. The full information on the system parameters and the discovery is reported in Liu et al. (2019).

Since the publication of the discovery paper, there are a number of studies that attempt either to reject specific formation scenarios of LB-1 (the massive BH is the BH-BH merger product or a very close BH-BH binary; see Shen et al. 2019) or to explain it with some specific scenarios: stellar evolution of a massive magnetic star (Groh et al. 2019), merger of two unevolved stars (Tanikawa et al. 2019), merger of a BH and an unevolved star (Banerjee 2019; Olejak et al. 2019). It was also pointed out that the existence of LB-1 (and its future evolution) may be in tension with the non-detection of ultra-luminous X-ray sources or black hole neutron star systems in the Galaxy (Safarzadeh et al. 2019). Alternatively, the nature of LB-1 is questioned with a reanalysis of observational data and results that support the idea that either the BH or both components are of lower mass than originally claimed (Abdul-Masih et al. 2019; El-Badry & Quataert 2019; Eldridge et al. 2019; Simón-Díaz et al. 2019; Irrgang et al. 2019). This would allow the classical isolated binary evolution at high metallicity to explain the formation of LB-1.

In fact, the existence of a 70 $M_{\odot}$ BH in high metallicity environment seems challenging. The current consensus is based on mass loss rate estimates and their dependence on metallicity for H-rich stars (Vink et al. 2001) and He-rich stars (Vink & de Koter 2005; Sander et al. 2019) that seems to limit BH mass to about 20 $M_{\odot}$ at solar metallicity (Belczynski et al. 2010). Existing electromagnetic observations seem to support this paradigm (Casares & Jonker 2014). Note the masses of the two most massive stellar-origin BHs that are known to have formed at relatively high metallicity are the well known Cyg X-1 ($M_{\rm BH} = 14.8 \pm 1.0$ $Z \approx 0.02$; Orosz et al. 2011) and M33 X-7 ($M_{\rm BH} = 15.7 \pm 1.5$, $Z \approx 0.1\,Z_{\odot}$; Valsecchi et al. 2010).

The mass of the BH in LB-1 seems to contradict pair-instability pulsation supernovae (PPSN) and pair-instability supernova (PSN) theory, that limits BH mass to about $M_{\rm BH} < 40 - 50$ $M_{\odot}$ (Bond et al. 1984; Heger & Woosley 2002; Woosley 2017; Farmer et al. 2019; Leung et al. 2019). This limit was recently proposed to be as high as ~ 55 $M_{\odot}$ for non-zero metallicity stars (Population I/II) by Belczynski et al. (2017). Note that for the LIGO/Virgo most massive BH-BH merger in O1/O2 (GW170729), the primary BH mass was reported to be 51.2 $M_{\odot}$. This high mass (not the merger itself) is likely to be a statistical fluctuation (Fishbach et al. 2019). However, even such mass can be explained as long as the BH was formed at low metallicity. The PPSN/PSN instability can be avoided (at best) for a 70 $M_{\odot}$ star that can possibly produce 69 $M_{\odot}$ BH if only small neutrino mass loss takes place at the BH formation. This was envisioned for an ultra-low metallicity and Population III stars as they can keep massive H-rich envelopes (Heger & Woosley 2002; Woosley 2017).

Here, we propose that a similar mechanism may also work at high metallicity. The modification that we need to introduce to stellar evolution is to lower wind mass loss rates for (at least some) massive stars. The empiric diagnostics of winds of the massive stars are complex, especially because of the wind clumping (Fullerton et al. 2006; Oskinova et al. 2007) and the agreement between theory and observations are not always conclusive (Keszthelyi et al. 2017).

In lower metallicity environments, such as in the LMC and the SMC galaxies, some work (Massa et al. 2017) indicates that wind mass loss rates may be actually higher than typically adopted in evolutionary predictions (Vink et al. 2001; Belczynski et al. 2010), others seem to agree with standard calculations (Ramírez-Agudelo et al. 2017), and yet others point out to much lower mass-loss rates than expected (Bouret et al. 2003; Ramachandran et al. 2019; Sundqvist et al. 2019). In the upper stellar mass regime, Hainich et al. (2013, 2019) determine mass-loss rates which are in broad agreement with the theoretical expectations.

In this work we consider the mass regime $70 - 100$ $M_{\odot}$ at solar metallicity. Vink & Gräfener (2012) have shown that for stars in transitional regime (from optically thin to thick winds) the standard mass loss rates should apply. The empirical studies that include hydrogen-rich Wolf-Rayet stars (Hamann et al. 2019) find mass-loss rates lower than theoretically predicted Nugis & Lamers (2000) for the most luminous objects. However, what are the mass-loss rates of such massive stars when they are very young is not well known. Gruner et al. (2019) found that the mass-loss rate of the earliest O-type star in the Galaxy (HD 93129A, the primary mass is ~ 100 $M_{\odot}$) compares well with the theoretical expectations, but this result depends on assumed clumping parameters. Furthermore, about 7% of OB stars are known to have (mostly) dipolar magnetic fields (Fossati et al. 2015; Wade et al. 2016; Grunhut et al. 2017). Some of these known magnetic stars are massive, but not quite reaching the mass regime considered here unless errors on mass estimates are considered: 61 ± 33 $M_{\odot}$ for CPD-28 2561 or ~ 60 $M_{\odot}$ for HD 148937 (David-Uraz et al. 2019). These magnetic fields may capture wind particles and reduce wind mass loss rates independent of star mass and metallicity (Owocki et al. 2016; Petit et al. 2017; Shenar et al. 2017; Georgy et al. 2017). Here we show two things. First, that the decrease of wind mass loss rates (independent of the reduction origin) allows some models to avoid pair-instability associated mass loss and allow for the formation of high mass BHs ($\sim 50 - 70$ $M_{\odot}$) at high metallicity. Second, that we are not able to make such a massive BH progenitor star fit within binary orbit of LB-1, if in fact LB-1 hosts a 70 $M_{\odot}$ BH.

2. CALCULATIONS

2.1. *Simple* `StarTrack` *Simulation*

We used the population synthesis code `StarTrack` (Belczynski et al. 2002, 2008) to quickly test the possibility of the formation of a 70 $M_{\odot}$ BH with decreased wind mass loss. We employed the rapid core-collapse supernova (SN) engine NS/BH mass calculation (Fryer et al. 2012), with strong PPSN/PSN mass loss (Belczynski et al. 2016). Standard winds for massive stars are used as the base model: O/B star Vink et al. (2001) winds and LBV winds (specific prescriptions for these winds are listed in Sec.2.2 of Belczynski et al. 2010). In wind mass loss prescriptions we introduce a multiplication factor that for our standard calculation is $f_{\rm wind} = 1.0$. Note that such approach produces a maximum of ~ 15 $M_{\odot}$ for BHs at high metallicity ($Z = 0.02$ assuming $Z_{\odot} = 0.017$) as demonstrated in Figure 1. We also calculate evolution of single stars for decreased winds for two extra models with $f_{\rm wind} = 0.5, 0.2$. It is clear from Figure 1 that winds need to be reduced by a factor of ~ 5 to produce a ~ 70 $M_{\odot}$ BH at high metallicity.

Our specific example is a star with $M_{\rm zams} = 104$ $M_{\odot}$ at $Z = 0.02$ and the star is evolved with Hurley et al. (2000) analytic formulae (used in many population syn-

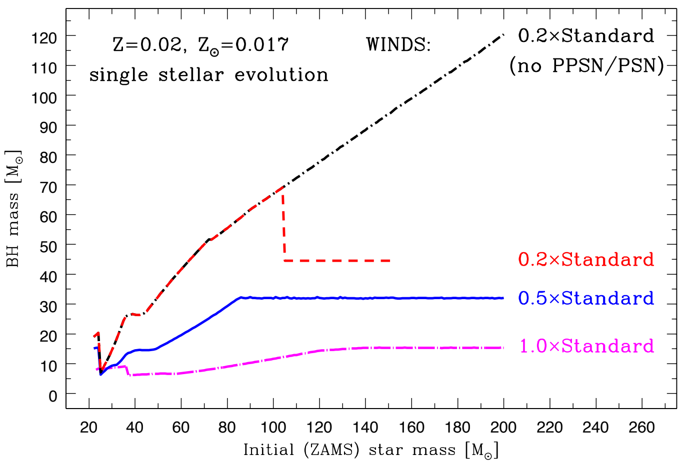

FIG. 1.— Black hole mass for single stars at metallicity estimated for LB-1 as a function of initial star mass. For standard wind mass loss prescriptions only low-mass black holes are predicted: $M_{\rm BH} < 15$ M$_\odot$. For reduced wind mass loss, however, much heavier black holes are formed: $M_{\rm BH} = 30$ M$_\odot$ for winds reduced by factor of 2, and $M_{\rm BH} = 70$ M$_\odot$ for winds reduced by factor of 5 of the standard values. Note that to reach even higher masses it is needed to switch off pair-instability pulsation supernovae that severely limit black hole masses.

thesis and globular cluster evolutionary codes). H-rich wind mass loss rates are decreased with $f_{\rm wind} = 0.2$. The star keeps its H-rich envelope throughout the entire evolution. After 3.8 Myr of evolution, the star has a mass of $M_{\rm tot} = 69.8$ M$_\odot$ with a H-rich envelope mass of $M_{\rm env} = 24.8$ M$_\odot$, He core mass of $M_{\rm He} = 44.99$ M$_\odot$, and CO core mass of $M_{\rm CO} = 34.8$ M$_\odot$. According to the simplistic population synthesis prescription (no PPSN/PSN for stars with $M_{\rm He} < 45.0$ M$_\odot$; Woosley 2017) this star is not yet the subject to PPSN/PSN. The star undergoes core-collapse and with 1% neutrino mass loss it forms a BH through direct collapse: $M_{\rm BH} = 69.1$ M$_\odot$.

2.2. *Single Star Evolutionary Models*

To explore the possibility of the LB-1 black hole being the descendant of a single star and to test the simple estimates from Section 2.1, we ran a series of stellar evolution models using the `MESA` code revision 11701 (Paxton et al. 2015). We used a solar initial composition of $Z = 0.014$ for all models with an Asplund et al. (2009) metal mixture (`initial_zfracs = 6`), and the corresponding opacity tables (`kappa_file_prefix = 'a09'`) including low-temperature tables (`kappa_lowT_prefix = 'lowT_fa05_a09p'`) and C/O-enhanced (type 2) opacity tables (`kappa_CO_prefix = 'a09_co'`). For convection, we used the Schwarzschild boundary location condition and included convective boundary mixing with a value of the exponentially-decaying diffusion coefficient parameter f and f_0 everywhere equal to 0.004. For the reaction network, we used the `basic.net` and `auto_extend_net = .true.`, with which `MESA` adapts the network along the evolution to the smallest network needed to trace energy generation. The main "stabilizing" setting/approximation was the use of extra pressure at the surface of the star by setting `Pextra_factor = 2`. Another one was the use of `MLT++` (see Paxton et al. 2013, Sect. 7). These settings might underestimate the radius of the star in our models. The models were evolved at least until the end of core He-burning and generally stopped due to convergence issues near the end of core carbon burning.

TABLE 1
INITIAL MASS, ROTATION AND MASS LOSS RE-SCALING FACTOR (COLUMNS 1-3) AND FINAL TOTAL, HE- AND CO-CORES MASSES AND MAXIMUM RADIUS (COLUMNS 4-7) OF THE STELLAR MODELS.

$M_{\rm zams}$	$\Omega/\Omega_{\rm crit}$	$f_{\rm wind}$	$M_{\rm tot}$	$M_{\rm He}$	$M_{\rm CO}$	$R_{\rm max}$/ R$_\odot$
Non-rotating models						
100	0.0	0.576	70.8	41.5	36.9	711.1
85	0.0	0.333	70.9	31.6	27.6	653.9
70	0.0	0.0	70.0	30.8	27.0	637.5
Rotating models						
100	0.6	0.576	61.6	49.5	43.9	260.8
85	0.6	0.576	58.2	40.3	35.4	363.9
85	0.6	0.333	62.9	46.8	41.3	235.0
75	0.6	0.576	53.9	34.5	30.1	376.5
70	0.6	0.576	50.2	32.1	27.8	324.1
70	0.4	0.282	58.5	32.5	28.3	611.8
Rotating models losing entire H-layer						
100	0.6	1.0	40.5	40.5	36.8	170.9
100	0.8	0.882	43.4	43.4	37.5	165.5

We used the "Dutch" scheme for mass loss with a default `Dutch_scaling_factor = 1.0`. The two main mass loss prescriptions experienced by our hydrogen-rich models are Vink et al. (2001) for hot stars and de Jager et al. (1988), which we used for the cool "Dutch" wind. In order to reduce the mass loss rates, we lowered the `Dutch_scaling_factor` by introducing a multiplication factor in front of wind mass loss rates and we changed it in wide range $f_{\rm wind} = 1.0 - 0.0$. We calculated non-rotating and rotating models (see Tab. 1). The standard rotation settings were used (Heger et al. 2000). Rotation is set on the zero-age main-sequence and the initial rotation rate, in terms of $\Omega/\Omega_{\rm crit}$, is given in Table 1. We include the following rotation-induced instabilities; Eddington-Sweet circulation, secular shear instability and Taylor-Spruit dynamo (Spruit 2002). Table 1 gives key properties of representative stellar models. Using the physical ingredients described above and considering that the main uncertainty in the models is mass loss, we reduced the mass loss with a multiplication factor given in the Table in an attempt to produce a final total mass equal to that of LB-1, i. e. around 70 M$_\odot$.

Considering first non-rotating models, a model without mass loss ($M_{\rm zams} = 70$ M$_\odot$, $f_{\rm wind} = 0.0$) is also included for reference as the most extreme (and unrealistic) case. With th re-scaled wind by $f_{\rm wind} = 0.576$, a model with an initial mass of 100 M$_\odot$ ends with a total mass 70.8 M$_\odot$. This model has final core masses that will experience pair-instability pulsation mass loss, however, and thus lose more mass before it produces a BH. Furthermore, its radius is too large to fit in the orbit of LB-1. The most interesting model is the $M_{\rm zams} = 85$ M$_\odot$ with $f_{\rm wind} = 0.333$. The final total mass is 70.9 M$_\odot$ and very importantly the final CO core mass is below the limit for pair-instability pulsation supernova mass loss. Indeed, the CO core mass of this model is $M_{\rm CO} = 27.6$ M$_\odot$ (see Fig. 2), which is below the CO core mass threshold for PPSN according to Table 1 in Woosley (2017, no pulsations for models with CO core masses below 28 M$_\odot$). It is thus possible for this model to produce a 70 M$_\odot$ BH. Unfortunately, the maximum radius of this model ($R_{\rm max} \approx 650$ R$_\odot$; see Fig. 3) is too large to fit in Roche lobe of the LB-1's BH (< 200 R$_\odot$) and this model thus cannot provide a full solution for the origin of LB-1.

Considering rotating models, rotation-induced mixing leads to more massive cores and more mass loss (e.g., Hirschi et al. 2004). Thus the rotating models with similar initial parameters end with smaller total masses and larger core masses, which makes them less suitable candidates to explain LB-1. The only advantage of rotating models over non-rotating ones is that they end with smaller radii that could possibly fit in the LB-1. So we may then ask the question: what is the most massive final single star model that would always fit in LB-1? Considering models that lose the entire H-rich layers (e.g. 100 M$_\odot$ models at the bottom of Tab. 1) or pure He-star models of Woosley (2017) or Farmer et al. (2019), BH masses up to $45 - 50$ M$_\odot$ can be produced. Since He-stars are very compact, these would fit within the LB-1 BH Roche lobe but the BH mass would be below the current lower mass limit of 55 M$_\odot$ for LB-1. We also consider rotating models with $f_{\rm wind} = 0.576$ that do not lose H-rich layers: $M_{\rm zams} = 70, 75, 85, 100$ M$_\odot$. The 70 M$_\odot$ model has a final CO core mass below the pair-instability pulsation mass range so is likely to collapse to a BH with little mass loss. The final radius, however is not so small ($R_{\rm max} = 324$ R$_\odot$) and that model would not fit in Roche lobe of LB-1's primary and the total mass is smaller than the lower mass estimate of BH mass in LB-1. The 75 and 85 M$_\odot$ have a larger final masses but also larger CO core masses and radii so will likely lose some mass by pair-instability supernova pulsations and would not fit in LB-1. The 100 M$_\odot$ model produces relatively small maximum radius ($R_{\rm max} = 261$ R$_\odot$) but still it would not fit in Roche lobe of LB-1's primary. Although final model mass is large (above lower limit on LB-1 BH mass), this model has a massive CO core and is subject to strong pair-instability pulsation supernova mass loss. A similar case is found for 85 M$_\odot$ rotating model with $f_{\rm wind} = 0.333$. It thus seems very unlikely for a single star or a non-interacting star in a binary system to produce the BH in LB-1 with the currently derived properties.

3. DISCUSSION AND CONCLUSIONS

It is generally believed that Population I/II stars cannot form BHs in the mass range $\sim 55 - 135$ M$_\odot$, the so-called the second mass gap, due to mass loss in pair-instability pulsation supernovae and due to total star disruption by pair-instability supernovae. It was noted, however, that in one specific case the lower bound of the second mass gap can be shifted to ~ 70 M$_\odot$. Such case was proposed for metal-poor (Population III) stars, for which wind mass loss is negligible even for high mass stars and then such stars can retain massive H-rich envelopes throughout their evolution. Retention of massive H-rich envelope allows a star to ignite a H-burning shell, which supports the outer stellar layers and helps density/temperature in stellar interior to avoid pair-instability regime (where adiabatic index becomes small $\gamma < 4/3$). In principle, one can imagine a stable (against PPSN/PSN) stellar configuration with 70 M$_\odot$ star at the core-collapse, with He core mass of $\lesssim 40$ M$_\odot$ and H-rich envelope of $\gtrsim 30$ M$_\odot$ for a metal-poor star (for which mass loss is expected to be low, at least lower than at high metallicity).

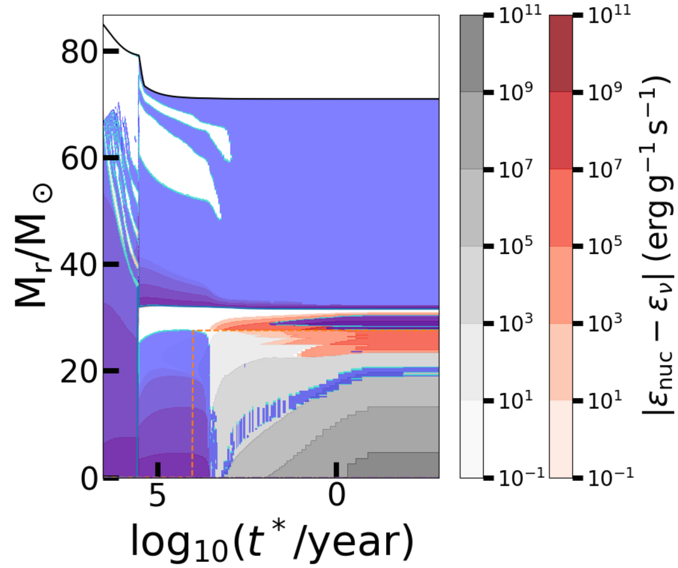

FIG. 2.— Stellar evolution diagram of the $M_{\rm zams} = 85$ M$_\odot$ non-rotating model with low stellar winds (reduced by a factor of 3 compared to the default) at $Z = 0.014$. The blue regions show the convective regions. Red shading indicates nuclear energy generation and grey shading indicates regions where cooling by neutrino emission dominates. The evolution of the star is presented as a function t^*, the time left until collapse/last model. The diagram presents the end of core hydrogen burning (left side), core helium burning and carbon burning (purple right). The top black solid lines indicates the total mass and the red dashed line indicates the He-free/poor core (defined as region where mass fraction of He is less than one percent). This model produces a 70.9 M$_\odot$ star at core collapse with a He core of $M_{\rm He} = 31.6$ M$_\odot$ and CO core of $M_{\rm CO} = 27.6$ M$_\odot$ and is most likely not subject to pair-instability pulsation supernova mass loss. This model can thus form a 70 M$_\odot$ black hole if there is no mass loss at BH formation.

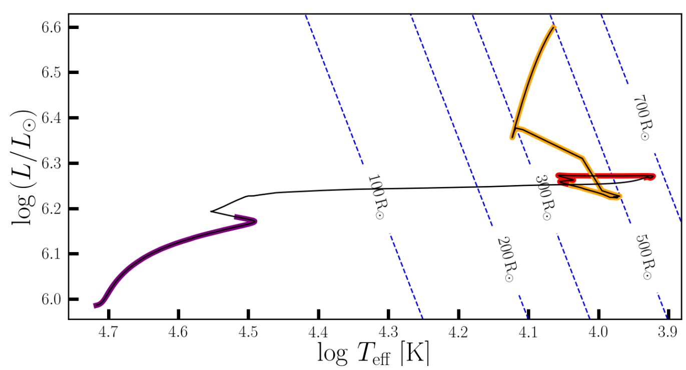

FIG. 3.— Hertzsprung-Russell diagram of the $M_{\rm zams} = 85$ M$_\odot$ non-rotating model with reduced stellar winds (by a factor of 3 compared to default settings). The central burning phases are highlighted, with purple for hydrogen, red for helium and orange for carbon burning. The blue dashed lines indicate contours of constant radii. This model expands to a maximum radius of $R_{\rm max} \approx 650$ R$_\odot$ before it loses mass during He-burning.

We found that similar configuration can be achieved for high metallicity stars if wind mass loss rates are decreased in stellar evolution models. For one model, a non-rotating $M_{\rm zams} = 85$ M$_\odot$ and $Z = 0.014$ star, we can form a 70 M$_\odot$ BH as a single star or a binary component in a very wide non-interacting binary if standard wind mass loss rates are reduced by factor of ~ 5. This is rather surprising and unexpected result on its own. Note that this result is totally independent of LB-1 and its true nature; whether it hosts a massive BH or not. This model, however, is not useful in context of LB-1 as the stellar radius of this star ($\gtrsim 650$ $R_\odot$) is too large to fit within LB-1 orbit.

The main uncertainty in the massive star models is mass loss. We reduced the mass loss rates in order to produce higher final masses. Note that reduced wind mass loss does not have to operate for all stars, but maybe it is possible that wind is quenched only for some fraction of very massive stars (e.g., via magnetic capture of wind particles: see Sec. 1). Other studies (e.g., Limongi & Chieffi 2018; Chieffi & Limongi 2019), however, show that a higher mass loss is needed in the red supergiant (RSG) phase to reproduce the absence of observed type II SNe above a certain luminosity (Smartt 2009). Evolved massive stars are also expected to lose mass via eruptive events, e.g. LBV-type mass loss, beyond the Humphreys-Davidson limit (Humphreys & Davidson 1979; Langer 2012; Smith 2014). These extra mass loss was suggested to explain the apparent lack of cool luminous massive stars in Milky Way (Mennekens & Vanbeveren 2014). Note that our model of non-rotating 85 $M_\odot$ star that can produce 70 $M_\odot$ BH enters cool ($\log_{10}(T_{\rm eff}) \approx 3.9$) and luminous ($\log_{10}(L/L_\odot) \approx 6.3$) region part of H-R diagram (see. Fig. 3). Even at low metallicity of Small Magellanic Cloud stars are not found at such low temperatures and such high luminosities (see Fig.13 of Ramachandran et al. (2019)).

Therefore, the existence of LB-1, if it really hosts a massive 70 $M_\odot$ BH, points to some other possibilities. *(i)* Either pair-instability does not operate in stars as expected. This would allow a rapidly rotating massive star to evolve homogeneously keeping small radius and forming 70 $M_\odot$ helium-rich object that would directly collapse to a black hole. *(ii)* Or the BH is a descendant of BH-BH or BH-star merger in inner binary and LB-1 was originally a triple system. Note that this would also require homogeneous evolution of two $\sim 30-50$ $M_\odot$ stars as not to affect nearby B star, but this would not require violating pair-instability theory. However, a gravitational-wave kick during BH-BH merger or any natal kick at BH formation, may be incompatible with very low eccentricity of LB-1. *(iii)* Maybe some stars expand less due to exotic composition and modifications of opacities or to an unknown additional mixing process. Alternatively, LB-1 may have lower mass components than claimed in the discovery paper and then standard stellar/binary evolution can account for the formation of such system.

Note that if BHs as massive as 70 $M_\odot$ exist in young and metal-rich environments, e.g., Galactic disk, they would most likely have low spins since our models employ effective angular momentum transport by magnetic dynamo ($a \lesssim 0.15$; see Belczynski et al. 2017). If such massive BH could catch a companion, e.g., in an open cluster, or have formed in a wide binary with another BH that then evolves into close/merging system, e.g., by a "lucky" natal kick injection into short period and eccentric orbit, then LIGO/Virgo will sooner or later discover these massive BHs. LIGO/Virgo detection of objects of such mass will be burdened with large errors, $\sim 20-30$ $M_\odot$ up and down, so in principle even a detection of a 100 $M_\odot$ BH could be possibly explained by one of our models.

Authors would like to thank Lida Oskinova and anonymous reviewer for useful comments. KB acknowledges support from the Polish National Science Center (NCN) grant Maestro (2018/30/A/ST9/00050). KB and RH acknowledge support from the World Premier International Research Center Initiative (WPI Initiative), MEXT, Japan. RH and EK acknowledge support from the ChETEC COST Action (CA16117), supported by COST (European Cooperation in Science and Technology). AH acknowledges support from the National Science Foundation under Grant No. PHY-1430152 (JINA Center for the Evolution of the Elements) and from the Australian Research Council Centre of Excellence for All Sky Astrophysics in 3 Dimensions (ASTRO 3D), through project number CE170100013. JC acknowledges support by the Spanish Ministry of Economy, Industry and Competitiveness (MINECO) under grant AYA2017-83216-P.

REFERENCES

Abdul-Masih, M., et al. 2019, arXiv e-prints, arXiv:1912.04092
Asplund, M., Grevesse, N., Sauval, A. J., & Scott, P. 2009, ARA&A, 47, 481
Banerjee, S. 2019, arXiv e-prints, arXiv:1912.06022
Belczynski, K., Bulik, T., Fryer, C. L., Ruiter, A., Valsecchi, F., Vink, J. S., & Hurley, J. R. 2010, ApJ, 714, 1217
Belczynski, K., Kalogera, V., & Bulik, T. 2002, ApJ, 572, 407
Belczynski, K., Kalogera, V., Rasio, F. A., Taam, R. E., Zezas, A., Bulik, T., Maccarone, T. J., & Ivanova, N. 2008, ApJS, 174, 223
Belczynski, K., et al. 2016, A&A, 594, A97
—. 2017, arXiv e-prints
Bond, J. R., Arnett, W. D., & Carr, B. J. 1984, ApJ, 280, 825
Bouret, J. C., Lanz, T., Hillier, D. J., Heap, S. R., Hubeny, I., Lennon, D. J., Smith, L. J., & Evans, C. J. 2003, ApJ, 595, 1182
Casares, J., & Jonker, P. G. 2014, Space Sci. Rev., 183, 223
Chieffi, A., & Limongi, M. 2019, arXiv e-prints, arXiv:1911.08988
David-Uraz, A., et al. 2019, MNRAS, 483, 2814
de Jager, C., Nieuwenhuijzen, H., & van der Hucht, K. A. 1988, A&AS, 72, 259
El-Badry, K., & Quataert, E. 2019, arXiv e-prints, arXiv:1912.04185
Eldridge, J. J., Stanway, E. R., Breivik, K., Casey, A. R., Steeghs, D. T. H., & Stevance, H. F. 2019, arXiv e-prints, arXiv:1912.03599
Farmer, R., Renzo, M., de Mink, S. E., Marchant, P., & Justham, S. 2019, arXiv e-prints, arXiv:1910.12874
Fishbach, M., Farr, W. M., & Holz, D. E. 2019, arXiv e-prints, arXiv:1911.05882
Fossati, L., et al. 2015, A&A, 582, A45
Fryer, C. L., Belczynski, K., Wiktorowicz, G., Dominik, M., Kalogera, V., & Holz, D. E. 2012, ApJ, 749, 91
Fullerton, A. W., Massa, D. L., & Prinja, R. K. 2006, ApJ, 637, 1025
Georgy, C., Meynet, G., Ekström, S., Wade, G. A., Petit, V., Keszthelyi, Z., & Hirschi, R. 2017, A&A, 599, L5
Giesers, B., et al. 2018, MNRAS, 475, L15
Groh, J. H., Farrell, E., Meynet, G., Smith, N., Murphy, L., & Allan, A. 2019, arXiv e-prints, arXiv:1912.00994
Gruner, D., et al. 2019, A&A, 621, A63
Grunhut, J. H., et al. 2017, MNRAS, 465, 2432
Hainich, R., Ramachandran, V., Shenar, T., Sand er, A. A. C., Todt, H., Gruner, D., Oskinova, L. M., & Hamann, W. R. 2019, A&A, 621, A85
Hainich, R., Ruehling, U., & Hamann, W.-R. 2013, in Massive Stars: From alpha to Omega, 155
Hamann, W. R., et al. 2019, A&A, 625, A57
Heger, A., Langer, N., & Woosley, S. E. 2000, ApJ, 528, 368
Heger, A., & Woosley, S. E. 2002, ApJ, 567, 532
Hirschi, R., Meynet, G., & Maeder, A. 2004, A&A, 425, 649
Humphreys, R. M., & Davidson, K. 1979, ApJ, 232, 409
Hurley, J. R., Pols, O. R., & Tout, C. A. 2000, MNRAS, 315, 543
Irrgang, A., Geier, S., Kreuzer, S., Pelisoli, I., & Heber, U. 2019, arXiv e-prints, arXiv:1912.08338
Keszthelyi, Z., Puls, J., & Wade, G. A. 2017, A&A, 598, A4

Langer, N. 2012, ARA&A, 50, 107
Leung, S.-C., Nomoto, K., & Blinnikov, S. 2019, arXiv e-prints
Limongi, M., & Chieffi, A. 2018, ApJS, 237, 13
Liu, J., et al. 2019, Nature, 575, 618
Massa, D., Fullerton, A. W., & Prinja, R. K. 2017, MNRAS, 470, 3765
Mennekens, N., & Vanbeveren, D. 2014, A&A, 564, A134
Nugis, T., & Lamers, H. J. G. L. M. 2000, A&A, 360, 227
Olejak, A., Belczynski, K., Bulik, T., & Sobolewska, M. 2019, arXiv e-prints, arXiv:1908.08775
Orosz, J. A., McClintock, J. E., Aufdenberg, J. P., Remillard, R. A., Reid, M. J., Narayan, R., & Gou, L. 2011, ApJ, 742, 84
Oskinova, L. M., Hamann, W. R., & Feldmeier, A. 2007, A&A, 476, 1331
Owocki, S. P., ud-Doula, A., Sundqvist, J. O., Petit, V., Cohen, D. H., & Townsend, R. H. D. 2016, MNRAS, 462, 3830
Paxton, B., et al. 2013, ApJS, 208, 4
—. 2015, ApJS, 220, 15
Petit, V., et al. 2017, MNRAS, 466, 1052
Ramachandran, V., et al. 2019, A&A, 625, A104
Ramírez-Agudelo, O. H., et al. 2017, A&A, 600, A81
Safarzadeh, M., Ramirez-Ruiz, E., & Belczynski, K. 2019, arXiv e-prints, arXiv:1912.10456
Sander, A. A. C., Vink, J. S., & Hamann, W. R. 2019, MNRAS, 2641
Shen, R. F., Matzner, C. D., Howard, A. W., & Zhang, W. 2019, arXiv e-prints, arXiv:1911.12581
Shenar, T., et al. 2017, A&A, 606, A91
Simón-Díaz, S., et al. 2019, arXiv e-prints, arXiv:1912.07255
Smartt, S. J. 2009, ARA&A, 47, 63
Smith, N. 2014, ARA&A, 52, 487
Spruit, H. C. 2002, A&A, 381, 923
Sundqvist, J. O., Björklund, R., Puls, J., & Najarro, F. 2019, arXiv e-prints, arXiv:1910.06586
Tanikawa, A., Kinugawa, T., Kumamoto, J., & Fujii, M. S. 2019, arXiv e-prints, arXiv:1912.04509
Thompson, T. A., et al. 2019, Science, 366, 637
Valsecchi, F., Glebbeek, E., Farr, W. M., Fragos, T., Willems, B., Orosz, J. A., Liu, J., & Kalogera, V. 2010, Nature, 468, 77
Vink, J. S., & de Koter, A. 2005, A&A, 442, 587
Vink, J. S., de Koter, A., & Lamers, H. J. G. L. M. 2001, A&A, 369, 574
Vink, J. S., & Gräfener, G. 2012, ApJ, 751, L34
Wade, G. A., et al. 2016, MNRAS, 456, 2
Woosley, S. E. 2017, ApJ, 836, 244